# Metabolic parameters of pretreatment 2-[18F]fluoro-D-glucose positron emission tomography for prognosis in patients with gallbladder adenocarcinoma: a cohort study

Can Li[1#], Yanliang Dong[1#], Yue Pan[1,2], Yun Han[1,2], Jingfeng Zhang[1,2], Xiaohui Luan[1,2], Jiajin Liu[1], Xiaodan Xu[1], Zhiwei Guan[1], Guanyun Wang[1,3], Baixuan Xu[1]

[1]Department of Nuclear Medicine, The First Medical Center, Chinese PLA General Hospital, Beijing, China; [2]Graduate School, Chinese PLA General Hospital, Beijing, China; [3]Nuclear Medicine Department, Beijing Friendship Hospital, Capital Medical University, Beijing, China

*Contributions:* (I) Conception and design: C Li, Y Dong, G Wang, B Xu; (II) Administrative support: C Li, Y Dong, Y Pan, Y Han, J Zhang; (III) Provision of study materials or patients: C Li, Y Dong, X Luan, J Liu, X Xu; (IV) Collection and assembly of data: C Li, Y Dong, G Wang; (V) Data analysis and interpretation: C Li, Y Dong, Z Guan; (VI) Manuscript writing: All authors; (VII) Final approval of manuscript: All authors.

[#]These authors contributed equally to this work.

*Correspondence to:* Baixuan Xu, MD. Department of Nuclear Medicine, The First Medical Center, Chinese PLA General Hospital, No. 28 Fuxing Road, Haidian District, Beijing 100853, China. Email: xbx301@163.com; Guanyun Wang, MM. Department of Nuclear Medicine, The First Medical Center, Chinese PLA General Hospital, No. 28 Fuxing Road, Haidian District, Beijing 100853, China; Nuclear Medicine Department, Beijing Friendship Hospital, Capital Medical University, Xicheng District, Beijing, China. Email: 852791126@qq.com.

**Background:** The incidence of gallbladder adenocarcinoma (GBA) is relatively low, yet it exhibits a high degree of malignancy and a significantly low 5-year survival rate. The aim of this study was to investigate the prognostic value of pretreatment 2-[18F]fluoro-D-glucose positron emission tomography {2-[18F]FDG PET} parameters in predicting outcomes for patients with GBA.

**Methods:** In total, 67 patients with GBA who underwent 2-[18F]FDG PET/computed tomography (CT) before treatment were retrospectively analyzed at Chinese PLA General Hospital from January 2012 to June 2022. All patients were diagnosed by pathology, and their baseline characteristics and clinical data were collected. The metabolic PET parameters of the primary and metastatic lesions were measured, including the maximum and average standardized uptake values (SUVs), metabolic tumor volume (MTV), and total lesion glycolysis (TLG). The prognostic significance of metabolic parameters and other clinical variables was assessed using Cox proportional hazards regression models. Differences in progression-free survival (PFS) and overall survival (OS) in relation to metabolic parameters were examined using the Kaplan-Meier method.

**Results:** During a median follow-up period of 14.2 months, 43 patients (64.2%) experienced tumor recurrence or progression, and 38 patients (56.7%) died of cancer. In the univariate Cox regression analysis, liver parenchymal invasion (P=0.001), lymph node metastasis (P=0.007), distant metastases (P=0.049), tumor differentiation (P=0.028), surgery (P=0.014), carcinoembryonic antigen (CEA) level (P=0.030), carbohydrate antigen 19-9 (CA19-9) level (P=0.003), TLG (P=0.005), MTV (P<0.001), sum of the TLGs of the primary and metastatic lesions (total TLG, tTLG) (P=0.001), and sum of the MTVs of the primary and metastatic lesions (total MTV, tMTV) (P<0.001) were significant predictors of PFS. In multivariate analysis, MTV was an independent predictor of PFS [hazard ratio (HR) =2.785; 95% confidence interval (CI): 1.204–6.441; P=0.017]. In the univariate Cox regression analysis, liver parenchymal invasion (P=0.001), lymph node metastasis (P=0.027), distant metastases (P=0.036), tumor differentiation (P=0.047), surgery (P=0.002), neutrophil-to-lymphocyte ratio (NLR) (P=0.011), CEA level (P=0.036), CA19-9 level (P<0.001), TLG (P=0.007), MTV (P<0.001), tTLG (P=0.003), and tMTV (P<0.001) were significant predictors of OS. In the

multivariate analysis, higher CA19-9 levels >37 U/mL and a greater tMTV (HR =2.961; 95% CI: 1.092–8.024; P=0.033) were predictive of OS.

**Conclusions:** Our study results suggest that pretreatment 2-[18F]FDG PET parameters can not only assist in the diagnosis of patients with GBA but may also serve as predictive factors for the prognosis of these patients and should thus be applied in their treatment.

**Keywords:** Gallbladder adenocarcinoma (GBA); 2-[18F]fluoro-D-glucose positron emission tomography {2-[18F] FDG PET}; prognosis; survival; metabolic tumor volume (MTV)

## Introduction

Being a rare type of malignancy, gallbladder cancer (GBC) accounts for only 0.6% of all cancers globally in 2020 (1). GBC most commonly originates from the epithelium, and nearly 90% of GBCs are classified as gallbladder adenocarcinoma (GBA) (2,3). Because most patients with GBC are asymptomatic and the disease progresses rapidly, they are often diagnosed with advanced disease (3). The 5-year survival rate of patients with advanced GBC is less than 10% (4,5). The only curative treatment option (radical resection) is typically offered in nonlocally advanced cases and can improve the survival rate of patients with GBC (6). However, it should be noted that a large proportion of patients might experience relapse after radical resection (7,8).

At present, the survival prediction for patients with GBA is mainly based on the eighth edition of the staging guidelines for tumor-node-metastasis (TNM) defined in the American Joint Committee on Cancer (AJCC) staging system (9,10). However, staging can only be performed after surgery, for which only a minority of patients with GBA are eligible (11). Through noninvasive imaging, it is possible to identify imaging markers that can predict survival before treatment, inform risk stratification and personalized decision-making, and potentially assist in the selection of management strategies and the prognosis of patients with GBA.

2-[18F]fluoro-D-glucose positron emission tomography/ computed tomography {2-[18F]FDG PET/CT} is mainly used to detect local lymph node metastasis and distant metastasis in patients with GBC with other potentially resectable lesions (12,13). The metabolic parameters of 2-[18F]FDG PET, including maximum standardized uptake value (SUVmax), peak SUV (SUVpeak), total lesion glycolysis (TLG), metabolic tumor volume (MTV), and others, have been shown to have predictive value in the prognosis of various malignancies (14-17). However, research on the prognosis of 2-[18F]FDG PET in GBA is limited, and only the metabolic parameters of the primary lesion—not those related to metastatic lesions—have been examined (18). In our study, we assessed the prognostic value of pretreatment 2-[18F]FDG PET metabolic parameters, including those of the primary and metastatic lesions, in GBA. We present this article in accordance with the STROBE reporting checklist (available at https://qims.amegroups.com/article/view/10.21037/qims-23-1003/rc).

## Methods

### Patients

In this study, we reviewed the imaging data of all patients with GBA (n=103) who underwent 2-[18F]FDG PET/ CT at the Chinese PLA General Hospital from January 2012 to June 2022. The inclusion criteria for patients were as follows: (I) an age of 18 years or older; (II) complete imaging and clinical data; (III) a pathological diagnosis; and (IV) completion of pretreatment 2-[18F]FDG PET/ CT. Meanwhile, the exclusion criteria for patients were as follows: (I) presence of other inflammatory diseases or malignancy (including autoimmune disease and infection); (II) presence of any diseases that could lead to increased liver uptake (including chronic liver disease or primary sclerosing cholangitis); (III) receipt of surgery or chemotherapy before 2-[18F]FDG PET/CT; and (IV) absence of follow-up records. The patient's clinical data, including medical history (gallbladder polyps, gallstones, cholecystitis), TNM stage, tumor differentiation, laboratory examinations [neutrophil-to-lymphocyte ratio (NLR),
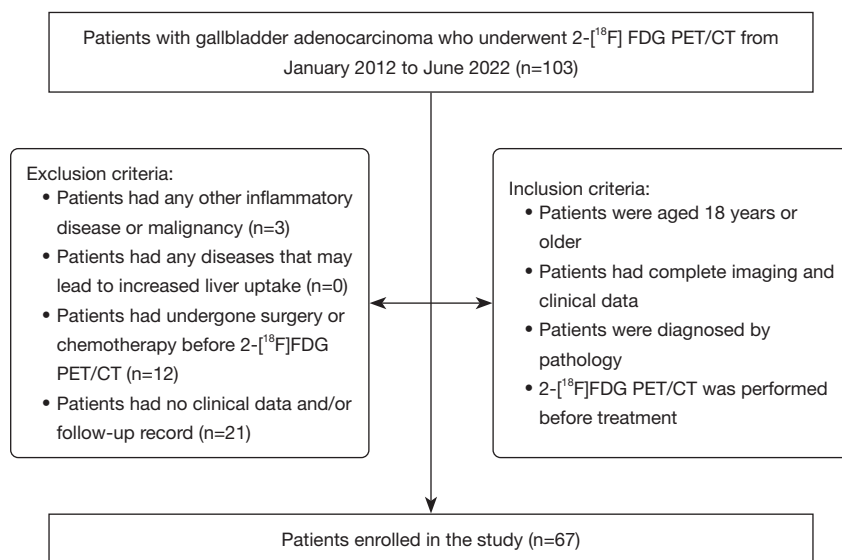
**Figure 1** Study flowchart of patient inclusion. 2-[$^{18}$F]FDG PET/CT, 2-[$^{18}$F]fluoro-D-glucose positron emission tomography/computed tomography.

carcinoembryonic antigen (CEA; ng/mL), carbohydrate antigen 19-9 (CA19-9; U/mL)], and treatment, were retrospectively collected from the clinical database of our hospital. The TNM stage was classified according to the AJCC manual, eighth edition (9). Based on the primary lesion, lymph node metastasis, and distant metastasis of the tumor in pathology and imaging, patients were classified into stage I, stage IIa, stage IIb, stage IIIa, stage IIIb, stage IVa, and stage IVb. The diagnosis of liver parenchyma invasion, lymph node metastasis, and distant metastasis mainly depended on the pathological results. For patients without pathological results, the evaluation was based on preoperative enhanced imaging examination, such as enhanced magnetic resonance imaging (MRI) or CT, and follow-up. The flowchart of patient inclusion and exclusion is shown in *Figure 1*.

This single-center, retrospective study was conducted in accordance with the Declaration of Helsinki (as revised in 2013) and approved by the local Ethics Committee of Chinese PLA General Hospital (No. S2014-052-01). The requirement for individual consent for this retrospective analysis was waived.

## 2-[$^{18}$F]FDG PET/CT image acquisition

After patients had fasted for at least 6 hours, their blood glucose levels were confirmed to be lower than 11.1 mmol/L before 2-[$^{18}$F]FDG (3.5–4.5 MBq/kg) was administered. Sixty minutes after the injection, all patients underwent 2-[$^{18}$F]FDG PET/CT performed with the Discovery 710 system (GE HealthCare, Chicago, IL, USA) or the Biograph 64 system (Siemens Healthineers, Erlangen, Germany). Whole-body CT images were obtained for attenuation correction using automatic dose modulation under the following settings: voltage, 120–140 kV; current, 100 mAs; rotation, 0.8; slice thickness, 3–5 mm; and pitch, 1 (19). Whole-body PET scans were obtained from the base of the skull to the upper femur in the free-breathing mode. The parameters of PET were three-dimensional mode, 2–2.5 min/bed (30% overlap), 4–5 beds/person, 3 iterations, 21 subsets, and a Gaussian filter half-height width of 4.0 mm.

## Image analysis

All images were reviewed by two experienced nuclear medical doctors (G.W. and C.L.) who were blinded to

the patients' clinical data and used commercially available imaging software (Advantage Workstation 4.6, GE HealthCare). None of the patients had any diseases that involved increased liver uptake, such as chronic liver disease or primary sclerosing cholangitis. The gallbladder region with abnormal 2-[$^{18}$F]FDG uptake on PET was defined as the primary lesion. Other regions with abnormal 2-[$^{18}$F]FDG uptake were considered metastatic lesions. All lesions were confirmed by surgical pathology and follow-up. We used software (Advantage Workstation 4.6, GE HealthCare) to automatically generate the contour around the target lesion within the boundary and manually depict the two-dimensional region of interest in combination with the contour within the contour edge to form the three-dimensional volume of interest (VOI). Contrast-enhanced MRI and CT were used to accurately determine the VOI. We applied a threshold of 40% of the SUVmax to select the lesions. The metabolic parameters of 2-[$^{18}$F]FDG PET were automatically generated by the software. Metabolic PET variables included the primary lesion SUVmax, primary lesion SUVpeak, primary lesion TLG [mean SUV (SUVmean) × MTV], primary lesion MTV, primary lesion tumor-to-normal liver SUV ratio (SUVR; SUVmax of the tumor/SUVmean of the normal liver parenchyma); SUVmax among the metastatic lesions (mSUVmax), SUVpeak among the metastatic lesions (mSUVpeak), SUVpeak among the metastatic lesions (mSUVpeak), sum of the TLGs of all metastatic lesions (mTLG), sum of the MTVs of all metastatic lesions (mMTV), sum of the TLG values of the primary and metastatic lesions (total TLG, tTLG), and sum of the MTVs of the primary and metastatic lesions (total MTV, tMTV).

There are some essential differences between the two PET/CT systems used in this study in terms of the machine design and scintillation detection that could lead to confusion concerning the SUVmax measurement results to some extent (20). To solve this issue, we retrospectively calculated the SUVmean of the liver parenchyma in the 67 patients from whom the original PET/CT images were available (GE Discovery 710: n=30; Siemens Biograph 64L n=37) (21). To measure normal liver parenchyma activity, three nonoverlapping spherical 1-cm$^3$ VOIs were drawn in the normal liver (liver 3/5/6 segments) on the axial PET images.

### Follow-up and prognosis

The progression-free survival (PFS) and overall survival (OS) were assessed for each patient. PFS was defined as the duration from the start of treatment to the detection of disease progression or the date of the last clinical follow-up. Disease progression was defined as an at least a 20% increase and 5-mm increase in the sum of the diameters of GBA lesions from baseline or the appearance of one or more new intragallbladder or extragallbladder metastatic lesions on follow-up imaging according to the revised Response Evaluation Criteria in Solid Tumors guidelines (version 1.1) (22). OS was defined as the interval between the first treatment and death from any cause or the final clinical follow-up.

### Statistical analysis

Categorical variables are expressed as number of cases and percentage. Continuous variables are expressed as medians with interquartile range (IQR). For statistical analyses, continuous variables, including age, NLR, and metabolic parameters, were dichotomized based on PFS results according to specific cutoffs, which were determined using receiver operating characteristic (ROC) curve analysis. Significant variables identified in the univariate Cox proportional hazard regression tests were included in the multivariate analysis. Due to there being significant correlations found among TLG, MTV, tTLG, and tMTV (P<0.001), only one metabolic parameter on 2-[$^{18}$F]FDG PET was included at a time in the multivariate analysis (23). Survival curves were generated using Kaplan-Meier estimates, and the log-rank test was used to assess the significance for PFS and OS. Statistical analysis was performed using SPSS 24.0 software (IBM, Armonk, NY, USA) and R 4.0.2 (The R Foundation for Statistical Computing). All statistical tests were two-sided, and P<0.05 indicated statistical significance.

## Results

### Patient characteristics

The baseline characteristics and clinicopathologic features of all enrolled patients are presented in *Table 1*. A total of 67 patients with GBA were enrolled in our study, including 25 men (37.3%) and 42 women (62.7%), with a median age of 63 years (IQR, 57–71 years). According to the AJCC staging system, 22 (32.8%), 31 (46.3%), and 14 patients (20.9%) had stage I/II, stage III, and stage IV disease, respectively. Among the patients, 38 (56.7%) had liver parenchyma

**Table 1** Patient clinical characteristics

| Characteristics | Value (n=67) |
|---|---|
| Age (years) | 63 [57–71] |
| Male sex | 25 (37.3) |
| Smoking history | 10 (14.9) |
| Drinking history | 6 (9.0) |
| Medical history | |
| Gallbladder polyps | 3 (4.5) |
| Gallstones | 8 (11.9) |
| Cholecystitis | 4 (6.0) |
| Stage | |
| I/II | 22 (32.8) |
| III | 31 (46.3) |
| IV | 14 (20.9) |
| Liver parenchymal invasion | 38 (56.7) |
| Lymph node metastasis | 39 (58.2) |
| Distant metastasis | 6 (9.0) |
| Tumor differentiation | |
| Well or moderate | 31 (46.3) |
| Poor | 36 (53.7) |
| Diagnostic method | |
| Surgical resection | 55 (82.1) |
| Needle biopsy | 12 (17.9) |
| Laboratory examination | |
| NLR | 2.3 [1.6–3.5] |
| CEA (ng/mL) | 3.0 [1.9–7.6] |
| CEA >5 ng/mL | 26 (38.8) |
| CA19-9 (U/mL) | 36.9 [14.5–687.4] |
| CA19-9 >37 U/mL | 33 (49.3) |
| Treatment | |
| Neoadjuvant therapy | 3 (4.5) |
| Surgery | 55 (82.1) |
| Primary tumor lesion | |
| SUVmax | 9.0 [6.2–14.7] |
| SUVpeak | 7.5 [5.1–12.2] |
| TLG | 77.9 [50.9–232.8] |
| MTV | 17.5 [12.0–34.4] |
| SUVR | 3.9 [2.7–6.4] |

Table 1 (*continued*)

**Table 1** (*continued*)

| Characteristics | Value (n=67) |
|---|---|
| Metastatic lesion (n=32) | |
| mSUVmax | 9.1 [6.2–9.1] |
| mSUVpeak | 7.0 [4.5–9.2] |
| mTLG | 59.4 [20.8–152.4] |
| mMTV | 10.6 [4.8–28.8] |
| Primary + metastatic lesions | |
| tTLG | 152.2 [52.1–366.6] |
| tMTV | 21.5 [14.6–41.2] |

Data are presented as n (%) or median [IQR]. NLR, neutrophil-to-lymphocyte ratio; CEA, carcinoembryonic antigen; CA19-9, carbohydrate antigen 19-9; SUVmax, maximum standardized uptake value; SUVpeak, peak standardized uptake value; TLG, total lesion glycolysis; MTV, metabolic tumor volume; SUVR, primary lesion tumor-to-normal liver standardized uptake value ratio; mSUVmax, SUVmax among the metastatic lesions; mSUVpeak, SUVpeak among the metastatic lesions; mTLG, sum of the TLGs of all metastatic lesions; mMTV, sum of the MTVs of all metastatic lesions; tTLG, total TLG, sum of the TLGs of the primary and metastatic lesions; tMTV, total MTV, sum of the MTVs of the primary and metastatic lesions.

invasion, 39 (58.2%) had lymph node metastasis, and 6 (9.0%) had distant metastasis. The diagnosis of 55 patients (82.1%) was based on surgical pathology, and 12 patients (17.9%) were diagnosed by needle biopsy. Of the 55 patients who underwent surgery, only 3 (4.5%) received neoadjuvant therapy before surgery. Concerning the degree of tumor differentiation, 31 patients (46.3%) had well- or moderately differentiated tumors, and 36 patients (53.7%) had poorly differentiated tumors. Regarding tumor markers, the median CEA level was 3.0 ng/mL (IQR, 1.9–7.6 ng/mL), and 26 patients (38.8%) had abnormal CEA levels (>5 ng/mL). The median CA19-9 level was 36.9 U/mL (IQR, 14.5–687.4 U/mL), and 33 patients (49.3%) had abnormal CA19-9 levels (>37 U/mL).

All patients were followed up for at least 1 year. During a median follow-up period of 14.2 months (IQR, 8.9–23.3 months), 43 patients (64.2%) experienced tumor recurrence or progression, and 38 patients (56.7%) died of cancer.

### *PET quantitative parameters*

We compared the liver parenchyma SUVmean of two

**Table 2** Cox univariate analyses of PFS

| Characteristics | Univariate analysis | |
| --- | --- | --- |
| | HR (95% CI) | P |
| Age (>63 years) | 1.385 (0.758–2.533) | 0.290 |
| Sex (male) | 1.291 (0.698–2.385) | 0.416 |
| Liver parenchymal invasion | 3.406 (1.688–6.872) | 0.001 |
| Lymph node metastasis | 2.509 (1.282–4.913) | 0.007 |
| Distant metastasis | 2.390 (1.003–5.696) | 0.049 |
| Poor tumor differentiation | 2.042 (1.078–3.867) | 0.028 |
| Neoadjuvant therapy | 0.694 (0.167–2.876) | 0.614 |
| Surgery | 0.408 (0.199–0.833) | 0.014 |
| NLR (>1.57) | 1.859 (0.861–4.017) | 0.114 |
| CEA (>5 ng/mL) | 1.963 (1.068–3.610) | 0.030 |
| CA19-9 (>37 U/mL) | 2.588 (1.371–4.887) | 0.003 |
| SUVmax (>4.75) | 2.791 (0.667–11.429) | 0.161 |
| SUVpeak (>3.91) | 2.519 (0.778–8.158) | 0.123 |
| TLG (>73.78) | 2.541 (1.331–4.851) | 0.005 |
| MTV (>30.73) | 3.620 (1.889–6.939) | <0.001 |
| SUVR (>1.43) | 22.517 (0.113–4495.82) | 0.249 |
| tTLG (>73.06) | 3.279 (1.597–6.735) | 0.001 |
| tMTV (>18.92) | 3.757 (1.845–7.649) | <0.001 |

PFS, progression-free survival; HR, hazard ratio; CI, confidence interval; NLR, neutrophil-to-lymphocyte ratio; CEA, carcinoembryonic antigen; CA19-9, carbohydrate antigen 19-9; SUVmax, maximum standardized uptake value; SUVpeak, peak standardized uptake value; TLG, total lesion glycolysis; MTV, metabolic tumor volume; SUVR, primary lesion tumor-to-normal liver standardized uptake value ratio; tTLG, total TLG, sum of the TLGs of the primary and metastatic lesions; tMTV, total MTV, sum of the MTVs of the primary and metastatic lesions.

different scanners, and there were no significant differences in terms of SUVmean of the liver between the two PET/CT scanners (GE Discovery 710: 2.33±0.46; Siemens Biograph 64: 2.38±0.47; P=0.671). The median SUVmax, SUVpeak, TLG, MTV, and SUVR were 9.0 (IQR, 6.2–14.7), 7.5 (IQR, 5.1–12.2), 77.9 (IQR, 50.9–232.8), 17.5 (IQR, 12.0–34.4), and 3.9 (IQR, 2.7–6.4), respectively. Of the 39 patients with lymph node metastasis and/or distant metastasis, metastatic lesions were found on 2-[$^{18}$F]FDG PET/CT in 32 patients (82.1%). The median mSUVmax, mSUVpeak, mTLG, and mMTV were 9.1 (IQR, 6.2–9.1),

7.0 (IQR, 4.5–9.2), 59.4 (IQR, 20.8–152.4), and 10.6 (IQR, 4.8–28.8), respectively. The median tTLG and tMTV were 152.2 (IQR, 52.1–366.6) and 21.5 (IQR, 14.6–41.2), respectively.

### Prognostic factors for PFS and OS

According to ROC analysis, the optimal cutoffs for age, NLR, SUVmax, SUVpeak, TLG, MTV, SUVR, tTLG, and tMTV for predicting PFS were 63 years, 1.57, 4.75, 3.91, 73.78, 30.73, 1.43, 73.06, and 18.92, respectively. In the univariate Cox regression analysis, liver parenchymal invasion, lymph node metastasis, distant metastasis, tumor differentiation, surgery, CEA and CA19-9 levels, TLG, MTV, tTLG, and tMTV were significant predictors of PFS (*Table 2*). Four multivariate models exhibited significant associations between metabolic parameters and PFS. In model 2, higher MTV (>30.73) was significantly associated with worse PFS [hazard ratio (HR) =2.785, 95% confidence interval (CI): 1.204–6.441; P=0.017; *Table 3*] after adjustments were made for liver parenchymal invasion, lymph node metastasis, distant metastases, tumor differentiation, surgery, and CEA and CA19-9 levels. Kaplan-Meier analysis of patients stratified by MTV revealed that patients with a higher MTV (>30.73) had worse PFS than did those with a lower MTV (log-rank =17.058; P<0.001; *Figure 2*).

According to ROC analysis, the optimal cutoffs for age, NLR, SUVmax, SUVpeak, TLG, MTV, SUVR, tTLG, and tMTV in predicting OS were 59 years, 1.62, 4.98, 3.91, 73.78, 21.03, 1.92, 73.06, and 18.92, respectively. In the univariate Cox regression analysis, liver parenchymal invasion, lymph node metastasis, distant metastasis, tumor differentiation, surgery, NLR, CEA and CA19-9 levels, TLG, MTV, tTLG, and tMTV were significant predictors of OS (*Table 4*). After adjustments were made for liver parenchymal invasion, lymph node metastasis, distant metastases, tumor differentiation, surgery, NLR, and CEA and CA19-9 levels, only one multivariate model (model 4) demonstrated a significant association between metabolic parameters and OS. In this model, higher tMTV (>18.92) was significantly associated with worse OS (HR =2.961; 95% CI: 1.092–8.024; P=0.033). Moreover, in all four models, higher CA19-9 levels (>37 U/mL) were associated with worse OS (model 1: HR =4.392, 95% CI: 1.754–10.997, P=0.002; model 2: HR =3.325, 95% CI: 1.260–8.772, P=0.015; model 3: HR =4.452, 95% CI:

610

Li et al. Prognostic value of PET in patients with GBA

**Table 3** Cox multivariate analyses of PFS

| Characteristics | Multivariate analysis (model 1) | | Multivariate analysis (model 2) | | Multivariate analysis (model 3) | | Multivariate analysis (model 4) | |
|---|---|---|---|---|---|---|---|---|
| | HR (95% CI) | P | HR (95% CI) | P | HR (95% CI) | P | HR (95% CI) | P |
| Liver parenchymal invasion | 1.811 (0.613–5.352) | 0.283 | 1.677 (0.539–5.215) | 0.372 | 1.620 (0.543–4.831) | 0.387 | 1.380 (0.443–4.297) | 0.579 |
| Lymph node metastasis | 1.153 (0.437–3.043) | 0.773 | 1.157 (0.425–3.153) | 0.775 | 1.128 (0.428–2.977) | 0.807 | 1.238 (0.458–3.349) | 0.674 |
| Distant metastasis | 1.892 (0.643–5.565) | 0.247 | 2.420 (0.799–7.323) | 0.118 | 1.967 (0.658–5.884) | 0.226 | 1.904 (0.633–5.729) | 0.252 |
| Poor tumor differentiation | 1.150 (0.531–2.491) | 0.723 | 1.297 (0.608–2.766) | 0.502 | 1.212 (0.568–2.586) | 0.619 | 1.252 (0.584–2.682) | 0.564 |
| Surgery | 1.001 (0.421–2.380) | 0.998 | 1.008 (0.435–2.332) | 0.986 | 1.026 (0.433–2.433) | 0.953 | 1.071 (0.451–2.547) | 0.876 |
| CEA (>5 ng/mL) | 1.483 (0.687–3.198) | 0.315 | 1.196 (0.529–2.704) | 0.668 | 1.456 (0.695–3.048) | 0.309 | 1.435 (0.675–3.051) | 0.348 |
| CA19-9 (>37 U/mL) | 1.771 (0.836–3.752) | 0.136 | 1.448 (0.625–3.214) | 0.363 | 1.772 (0.832–3.772) | 0.138 | 1.701 (0.806–3.589) | 0.163 |
| TLG (>73.78) | 1.551 (0.686–3.505) | 0.292 | – | – | – | – | – | – |
| MTV (>30.73) | – | – | 2.785 (1.204–6.441) | 0.017 | – | – | – | – |
| tTLG (>73.06) | – | – | – | – | 1.976 (0.857–4.558) | 0.110 | – | – |
| tMTV (>18.92) | – | – | – | – | – | – | 2.112 (0.890–5.011) | 0.090 |

PFS, progression-free survival; HR, hazard ratio; CI, confidence interval; CEA, carcinoembryonic antigen; CA19-9, carbohydrate antigen 19-9; TLG, total lesion glycolysis; MTV, metabolic tumor volume; tTLG, total TLG, sum of the TLGs of the primary and metastatic lesions; tMTV, total MTV, sum of the MTVs of the primary and metastatic lesions.
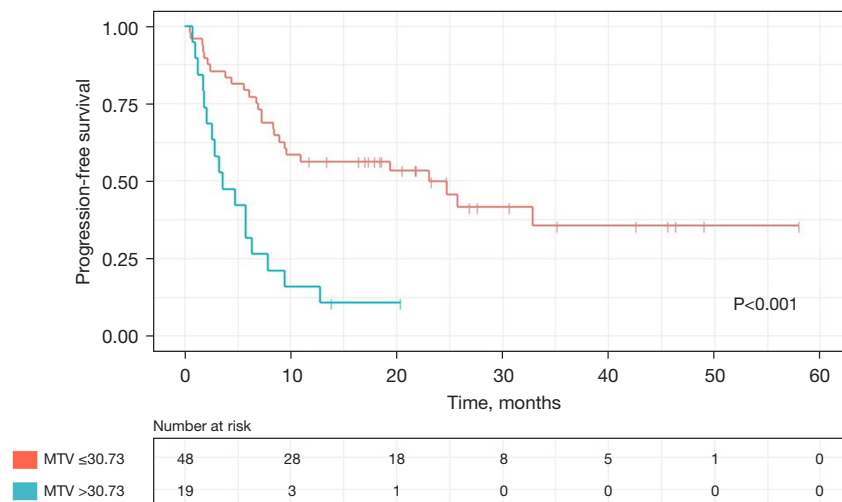


**Figure 2** Kaplan-Meier analysis of the relationship between PFS and MTV. MTV, metabolic tumor volume; PFS, progression-free survival.

**Table 4** Cox univariate and multivariate analyses of OS

| Characteristics | Univariate analysis | |
| --- | --- | --- |
| | HR (95% CI) | P |
| Age (>59 years) | 1.234 (0.612–2.488) | 0.558 |
| Sex (male) | 1.551 (0.807–2.979) | 0.188 |
| Liver parenchymal invasion | 3.875 (1.789–8.395) | 0.001 |
| Lymph node metastasis | 2.220 (1.094–4.505) | 0.027 |
| Distant metastasis | 2.553 (1.061–6.141) | 0.036 |
| Tumor differentiation (poor) | 1.992 (1.008–3.934) | 0.047 |
| Surgery | 0.317 (0.151–0.664) | 0.002 |
| Neoadjuvant therapy | 0.418 (0.057–3.060) | 0.391 |
| NLR (>1.62) | 3.411 (1.326–8.775) | 0.011 |
| CEA (>5 ng/mL) | 1.986 (1.047–3.768) | 0.036 |
| CA19-9 (>37 U/mL) | 5.190 (2.389–11.275) | <0.001 |
| SUVmax (>4.98) | 1.456 (0.447–4.745) | 0.533 |
| SUVpeak (>3.91) | 1.828 (0.561–5.950) | 0.317 |
| TLG (>73.78) | 2.588 (1.292–5.181) | 0.007 |
| MTV (>21.03) | 3.961 (1.990–7.887) | <0.001 |
| SUVR (>1.92) | 3.763 (0.515–27.467) | 0.191 |
| tTLG (>73.06) | 3.160 (1.472–6.785) | 0.003 |
| tMTV (>18.92) | 5.081 (2.264–11.405) | <0.001 |

OS, overall survival; HR, hazard ratio; CI, confidence interval; NLR, neutrophil-to-lymphocyte ratio; CEA, carcinoembryonic antigen; CA19-9, carbohydrate antigen 19-9; SUVmax, maximum standardized uptake value; SUVpeak, peak standardized uptake value; TLG, total lesion glycolysis; MTV, metabolic tumor volume; SUVR, primary lesion tumor-to-normal liver standardized uptake value ratio; tTLG, total TLG, sum of the TLGs of the primary and metastatic lesions; tMTV, total MTV, sum of the MTVs of the primary and metastatic lesions.

1.779–11.144, P=0.001; model 4: HR =4.653, 95% CI: 1.843–11.747, P=0.001; *Table 5*). Kaplan-Meier analysis of patients stratified by tMTV revealed that a higher tMTV (>18.92; log-rank =18.596; P<0.001) and a higher CA19-9 level (>37 U/mL; log-rank =20.985; P<0.001) were associated with worse OS (*Figure 3*).

## Discussion

In our study, we identified the metabolic parameters of 2-[$^{18}$F]FDG PET that are prognostic markers in patients with GBA. The MTV of the primary lesion could predict disease progression, and tMTV could predict death. CA19-9 was also valuable in predicting the death of patients with GBA.

GBC is an aggressive cancer with a poor prognosis (24). The survival rate of patients with advanced disease is extremely low even if extended cholecystectomy with lymph node resection and adjacent invasive organ resection are performed (25). In previous studies, age, sex, whole blood cell count, tumor markers, degree of tumor differentiation, AJCC staging, tumor location, and treatment methods could predict the prognosis of patients with GBC (10,11,26-28). In our study, among the clinically relevant prognostic markers, we found that CA19-9 (U/mL) was an independent risk factor for predicting the death of patients with GBA. CA19-9 is one of the most commonly used tumor markers in GBC. Yu *et al.* reported that CA19-9 levels gradually increased with increasing progression of GBC (29). Thus, CA19-9 might be useful in predicting the tumor burden in patients with GBC (30). CA19-9 has also been indicated to be a predictor of poor prognosis in GBC (31). In patients with GBA, a higher baseline CA19-9 level may indicate a more invasive tumor and the presence of metastasis. In our study, abnormal CA19-9 levels (>37 U/mL) were also associated with death but not recurrence or progression. Patients with GBA and abnormal baseline CA19-9 levels (>37 U/mL) demonstrated a shorter survival period Therefore, abnormal baseline CA19-9 levels may be predictive of survival in patients with GBA.

2-[$^{18}$F]FDG PET, as a molecular imaging technology, uses the glucose analog 2-[$^{18}$F]FDG to noninvasively display glucose consumption *in vivo*. 2-[$^{18}$F]FDG PET is widely used to reveal tumor glucose metabolism in a variety of tumors (32,33), for which it has also demonstrated predictive and prognostic value (34). 2-[$^{18}$F]FDG PET also holds clinical value in the diagnosis of primary tumors in GBC (35). Therefore, to identify those prognostic markers able to inform treatment decisions in patients with GBA, we investigated the prognostic value of the metabolic parameters of 2-[$^{18}$F]FDG PET in GBA and compared them with other clinical parameters. Several other studies have investigated the prognostic value of 2-[$^{18}$F]FDG PET parameters in patients with GBC. Furukawa *et al.* were the first to analyze the prognostic value of $^{18}$F-FDG PET SUV in biliary tract carcinomas including GBC (36). The results illustrated that SUV was helpful for predicting the prognosis in biliary tract carcinoma, with a higher SUVmax of the primary lesion as measured on pretreatment 2-[$^{18}$F]

**Table 5** Cox multivariate analyses of OS

| Characteristics | Multivariate analysis (model 1) | | Multivariate analysis (model 2) | | Multivariate analysis (model 3) | | Multivariate analysis (model 4) | |
|---|---|---|---|---|---|---|---|---|
| | HR (95% CI) | P | HR (95% CI) | P | HR (95% CI) | P | HR (95% CI) | P |
| Liver parenchymal invasion | 3.074 (0.921–10.262) | 0.068 | 2.347 (0.664–8.303) | 0.186 | 2.798 (0.813–9.625) | 0.103 | 2.149 (0.615–7.517) | 0.231 |
| Lymph node metastasis | 0.499 (0.173–1.442) | 0.199 | 0.596 (0.193–1.835) | 0.367 | 0.488 (0.168–1.416) | 0.187 | 0.544 (0.183–1.614) | 0.272 |
| Distant metastasis | 2.148 (0.686–6.719) | 0.189 | 3.477 (0.939–12.869) | 0.062 | 2.312 (0.721–7.414) | 0.159 | 2.332 (0.703–7.734) | 0.166 |
| Poor tumor differentiation | 0.802 (0.347–1.853) | 0.606 | 0.826 (0.361–1.890) | 0.651 | 0.863 (0.381–1.957) | 0.724 | 0.795 (0.343–1.841) | 0.592 |
| Surgery | 0.654 (0.266–1.610) | 0.356 | 0.622 (0.265–1.461) | 0.276 | 0.652 (0.268–1.586) | 0.346 | 0.758 (0.310–1.852) | 0.543 |
| NLR (>1.62) | 1.884 (0.688–5.157) | 0.217 | 1.592 (0.565–4.486) | 0.337 | 1.753 (0.638–4.820) | 0.277 | 1.726 (0.626–4.759) | 0.291 |
| CEA (>5 ng/mL) | 1.224 (0.536–2.795) | 0.631 | 1.073 (0.470–2.447) | 0.867 | 1.258 (0.571–2.768) | 0.569 | 1.036 (0.455–2.362) | 0.933 |
| CA19-9 (>37 U/mL) | 4.392 (1.754–10.997) | 0.002 | 3.325 (1.260–8.772) | 0.015 | 4.452 (1.779–11.144) | 0.001 | 4.653 (1.843–11.747) | 0.001 |
| TLG (>73.78) | 1.475 (0.597–3.645) | 0.399 | – | – | – | – | – | – |
| MTV (>30.73) | – | – | 2.561 (0.903–7.262) | 0.077 | – | – | – | – |
| tTLG (>73.06) | – | – | – | – | 2.961 (1.092–8.024) | 0.033 | – | – |
| tMTV (>18.92) | – | – | – | – | – | – | 2.961 (1.092–8.024) | 0.033 |

OS, overall survival; HR, hazard ratio; CI, confidence interval; NLR, neutrophil-to-lymphocyte ratio; CEA, carcinoembryonic antigen; CA19-9, carbohydrate antigen 19-9; TLG, total lesion glycolysis; MTV, metabolic tumor volume; tTLG, total TLG, sum of the TLGs of the primary and metastatic lesions; tMTV, total MTV, sum of the MTVs of the primary and metastatic lesions.
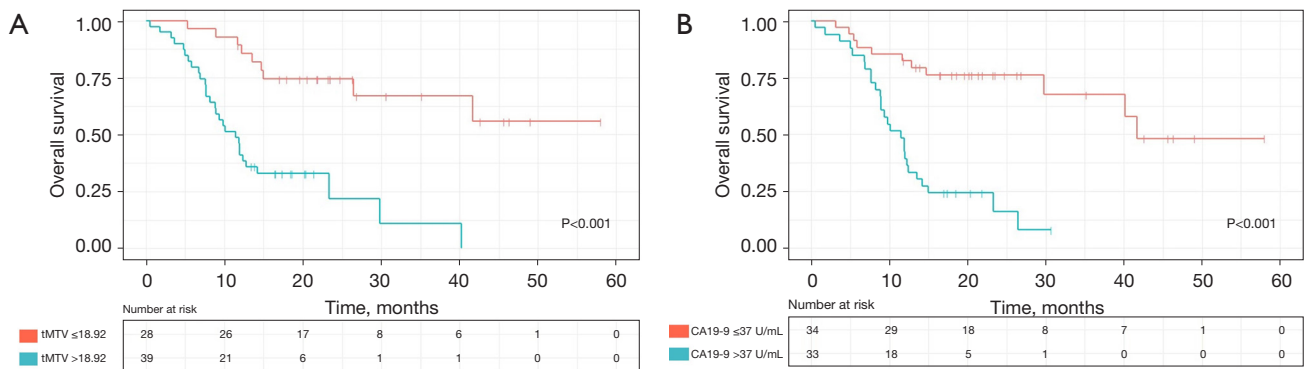


**Figure 3** Kaplan-Meier analysis of the relationship of OS with the (A) tMTV and (B) CA19-9. tMTV, total MTV, sum of the MTVs of the primary and metastatic lesions; MTV, metabolic tumor volume; CA19-9, carbohydrate antigen 19-9; OS, overall survival.

FDG PET being associated with worse survival rates. SUVmax represents the highest glucose uptake in the tumor or normal tissues, and it is the most common semiquantitative parameter of 2-[$^{18}$F]FDG PET. However, our results did not indicate that SUVmax and SUVR are related to the prognosis of patients with GBA. Quantitative metabolic activity can provide valuable information for tumor diagnosis and help predict and evaluate the therapeutic response in clinical oncology (37). MTV and TLG can represent tumor volume and glucose activity and reflect the glucose metabolism state of tumor tissues (38). Yoo *et al.* studied the prognostic value of volume-based metabolic parameters in 2-[$^{18}$F]FDG PET/CT for patients with GBC in comparison with other prognostic parameters. The results revealed that TLG of the primary tumor and the clinical or pathological TNM stage were significant independent prognostic factors for OS in patients with GBC (39). In our study, we found that TLG and MTV of the primary lesion were significantly associated with PFS in univariate analysis, but in multivariate analysis, only the MTV of the primary lesion was an independent risk factor for PFS in patients with GBA. Increases in the value of 2-[$^{18}$F]FDG PET metabolic parameters based on the primary tumor volume reflect increases in malignancy and invasiveness in GBA, which in turn may affect prognosis.

Because of the nonspecific clinical manifestations and histological structure of the gallbladder, GBC is inclined toward adjacent organ invasion, lymph node metastasis, and distant metastasis (40,41). Consequently, GBC is often diagnosed at an advanced stage. Therefore, adding volume-based 2-[$^{18}$F]FDG PET metabolic parameters of metastatic lesions to those of primary lesions might reflect patients' overall tumor burden before treatment and potentially better predict patients' prognosis. Kim *et al.* analyzed the prognostic value of the quantitative parameters of 2-[$^{18}$F]FDG PET/CT, including tMTV and tTLG, in patients with locally advanced and metastatic GBC (32). The results demonstrated that tMTV could identify patients with poor prognosis. The aforementioned study results are consistent with our findings, specifically that in which tMTV was found to be an independent risk factor for death in patients with GBA; however, it was not an independent risk factor for recurrence and progression. When 2-[$^{18}$F]FDG PET indicates a higher tMTV in patients with GBA before treatment, this suggests that the patient has a larger lesion, a wider invasion range, and a greater likelihood of metastasis (*Figure 4*). Therefore, an excessive tumor burden before treatment might indeed lead to shortened survival, and patients with GBA and a higher tMTV tend to have a shorter survival period. Pretreatment 2-[$^{18}$F]FDG PET can detect a greater number of metastatic lesions in patients with GBA to more accurately assist in staging and evaluating treatment efficacy. In addition, the results of our study demonstrate that 2-[$^{18}$F]FDG PET can also aid in predicting prognosis in patients GBA.

Our present study had several limitations. First, we employed a single-center, retrospective study design with a small number of patients. However, compared with previous studies, we only analyzed patients with GBA, and all patients were diagnosed via pathological results. Second, we used ROC to select the optimal cutoffs of 2-[$^{18}$F]FDG PET metabolic parameters, which could lead to the inconsistent selection of 2-[$^{18}$F]FDG PET metabolic parameters under different conditions. It is thus necessary to identify accurate cutoffs in larger numbers of patients. Third, the measurement of metabolic parameters should account for the influence of multiple factors, such as blood glucose and insulin levels. Fourth, because of the variability in patients' conditions, some relevant clinical prediction parameters were not included in our study. In the future, we will conduct a prospective study with a larger sample size and include more relevant predictive variables to ensure the accuracy of the research.

## Conclusions

The metabolic parameters of 2-[$^{18}$F]FDG PET are related to the prognosis of patients with GBA. PET-derived parameters including primary lesion TLG, primary lesion MTV, tTLG, and tMTV were significantly associated with PFS and OS in patients with GBA. Importantly, MTV of the primary lesion independently predicted PFS in multivariate analysis. CA19-9 level (>37 U/mL) and tMTV independently predicted OS in multivariate analysis. Pretreatment 2-[$^{18}$F]FDG PET metabolic parameters can be used as prognostic markers in GBA and thus may be valuable for risk stratification and treatment management.
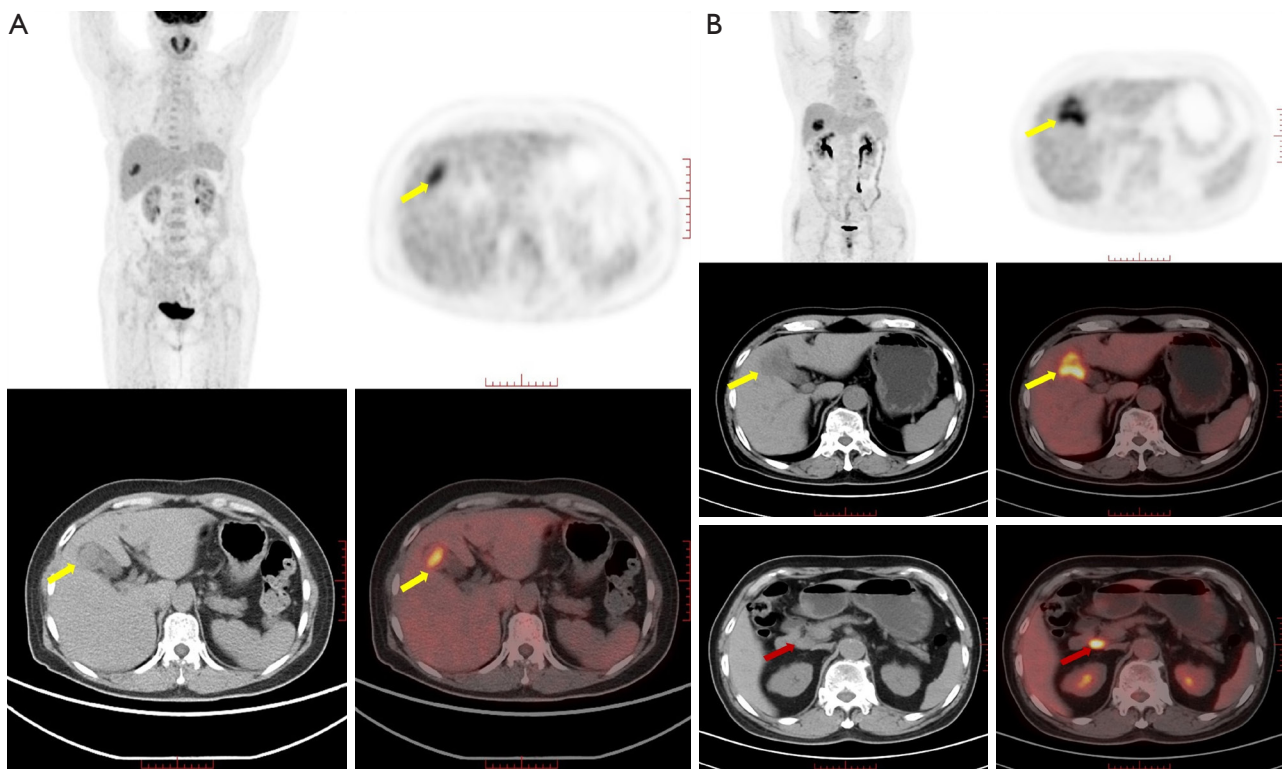
**Figure 4** Images of the patients. (A) A 57-year-old woman who was diagnosed with poorly differentiated adenocarcinoma without invasion of the liver parenchyma, lymph node metastasis, or distant metastasis. MIP images revealed a lesion with high uptake in the gallbladder region, but no metastatic lesions were found. The yellow arrow denotes a mass with a slightly elevated density in the gallbladder region and high 2-[$^{18}$F]FDG uptake. The MTV of the primary lesion and tMTV were both 15.14. The patient was alive without recurrence at the end of follow-up. (B) A 72-year-old man who was diagnosed with poorly differentiated GBA with invasion of the liver parenchyma and lymph node metastasis via surgical pathology. MIP images revealed a lesion with high uptake in the gallbladder with intraperitoneal lymph node metastasis. The yellow arrow denotes a mass with uneven density in the gallbladder region, an unclear boundary with the adjacent liver parenchyma, and high 2-[$^{18}$F]FDG uptake. The red arrow denotes a metastatic lymph node with high uptake in the hilar region. MTV of the primary lesion was 33.54, and tMTV was 38.84. The patient experienced recurrence 5.8 months after surgery and died 1 year later. MIP, maximum intensity projection; 2-[$^{18}$F]FDG, 2-[$^{18}$F]fluoro-D-glucose; tMTV, total MTV, sum of the MTVs of the primary and metastatic lesions; GBA, gallbladder adenocarcinoma; MTV, metabolic tumor volume.

## Footnote

*Ethical Statement:* The authors are accountable for all aspects of the work in ensuring that questions related to the accuracy or integrity of any part of the work are appropriately investigated and resolved. This single-center,

retrospective study was conducted in accordance with the Declaration of Helsinki (as revised in 2013) and was approved by the local Ethics Committee of Chinese PLA General Hospital (No. S2014-052-01). The individual consent for this retrospective analysis was waived.

## References

1. Sung H, Ferlay J, Siegel RL, Laversanne M, Soerjomataram I, Jemal A, Bray F. Global Cancer Statistics 2020: GLOBOCAN Estimates of Incidence and Mortality Worldwide for 36 Cancers in 185 Countries. CA Cancer J Clin 2021;71:209-49.

2. Bal MM, Ramadwar M, Deodhar K, Shrikhande S. Pathology of gallbladder carcinoma: current understanding and new perspectives. Pathol Oncol Res 2015;21:509-25.

3. Rakić M, Patrlj L, Kopljar M, Kliček R, Kolovrat M, Loncar B, Busic Z. Gallbladder cancer. Hepatobiliary Surg Nutr 2014;3:221-6.

4. Groot Koerkamp B, Fong Y. Outcomes in biliary malignancy. J Surg Oncol 2014;110:585-91.

5. Lee NK, Kim S, Moon JI, Shin N, Kim DU, Seo HI, Kim HS, Han GJ, Kim JY, Lee JW. Diffusion-weighted magnetic resonance imaging of gallbladder adenocarcinoma: analysis with emphasis on histologic grade. Clin Imaging 2016;40:345-51.

6. Wistuba II, Gazdar AF. Gallbladder cancer: lessons from a rare tumour. Nat Rev Cancer 2004;4:695-706.

7. Margonis GA, Gani F, Buettner S, Amini N, Sasaki K, Andreatos N, et al. Rates and patterns of recurrence after curative intent resection for gallbladder cancer: a multi-institution analysis from the US Extra-hepatic Biliary Malignancy Consortium. HPB (Oxford) 2016;18:872-8.

8. Kim TG. Patterns of initial failure after resection for gallbladder cancer: implications for adjuvant radiotherapy. Radiat Oncol J 2017;35:359-67.

9. Giannis D, Cerullo M, Moris D, Shah KN, Herbert G, Zani S, Blazer DG 3rd, Allen PJ, Lidsky ME. Validation of the 8th Edition American Joint Commission on Cancer (AJCC) Gallbladder Cancer Staging System: Prognostic Discrimination and Identification of Key Predictive Factors. Cancers (Basel) 2021.

10. Jiang S, Zhang J, Zhang L, Xu Y, Zhao H, Sang X, Lu X. A novel nomogram based on log odds of positive lymph nodes to predict survival for non-metastatic gallbladder adenocarcinoma after surgery. Sci Rep 2022;12:16466.

11. Xu B, Chen Z, Zhang J, Chang J, Zhao W, Dong Z, Zhi X, Li T. Prognostic Value of Peripheral Whole Blood Cell Counts Derived Indexes in Gallbladder Carcinoma: A Systematic Review and Meta-Analysis. Front Oncol 2021;11:707742.

12. Ramos-Font C, Gómez-Rio M, Rodríguez-Fernández A, Jiménez-Heffernan A, Sánchez Sánchez R, Llamas-Elvira JM. Ability of FDG-PET/CT in the detection of gallbladder cancer. J Surg Oncol 2014;109:218-24.

13. Lee SW, Kim HJ, Park JH, Park DI, Cho YK, Sohn CI, Jeon WK, Kim BI. Clinical usefulness of 18F-FDG PET-CT for patients with gallbladder cancer and cholangiocarcinoma. J Gastroenterol 2010;45:560-6.

14. Zer A, Domachevsky L, Rapson Y, Nidam M, Flex D, Allen AM, Stemmer SM, Groshar D, Bernstine H. The Role of 18F-FDG PET/CT on Staging and Prognosis in Patients with Small Cell Lung Cancer. Eur Radiol 2016;26:3155-61.

15. Memon S, Lynch AC, Akhurst T, Ngan SY, Warrier SK, Michael M, Heriot AG. Systematic review of FDG-PET prediction of complete pathological response and survival in rectal cancer. Ann Surg Oncol 2014;21:3598-607.

16. Im HJ, Zhang Y, Wu H, Wu J, Daw NC, Navid F, Shulkin BL, Cho SY. Prognostic Value of Metabolic and Volumetric Parameters of FDG PET in Pediatric Osteosarcoma: A Hypothesis-generating Study. Radiology 2018;287:303-12.

17. Gouw ZAR, La Fontaine MD, van Kranen S, van de Kamer JB, Vogel WV, van Werkhoven E, Sonke JJ, Al-Mamgani A. The Prognostic Value of Baseline 18F-FDG PET/CT in Human Papillomavirus-Positive Versus Human Papillomavirus-Negative Patients With Oropharyngeal Cancer. Clin Nucl Med 2019;44:e323-8.

18. Han YH, Jeong HJ, Lim ST. Clinical and metabolic parameters for predicting disease progression of gallbladder adenocarcinoma. Nucl Med Commun 2022;43:42-8.

19. Wang G, Zhang W, Chen J, Luan X, Wang Z, Wang Y, Xu

X, Yao S, Guan Z, Tian J, Lu S, Xu B, Ma G. Pretreatment Metabolic Parameters Measured by (18)F-FDG PET to Predict the Pathological Treatment Response of HCC Patients Treated With PD-1 Inhibitors and Lenvatinib as a Conversion Therapy in BCLC Stage C. Front Oncol 2022;12:884372.

20. Armstrong IS, Thomson KE, Rowley LM, McGowan DR. Harmonizing standardized uptake value recovery between two PET/CT systems from different manufacturers when using resolution modelling and time-of-flight. Nucl Med Commun 2017;38:650-5.

21. Hsieh CE, Cheng NM, Chou WC, Venkatesulu BP, Chou YC, Liao CT, Yen TC, Lin CY. Pretreatment Primary Tumor and Nodal SUVmax Values on 18F-FDG PET/CT Images Predict Prognosis in Patients With Salivary Gland Carcinoma. Clin Nucl Med 2018;43:869-79.

22. Eisenhauer EA, Therasse P, Bogaerts J, Schwartz LH, Sargent D, Ford R, Dancey J, Arbuck S, Gwyther S, Mooney M, Rubinstein L, Shankar L, Dodd L, Kaplan R, Lacombe D, Verweij J. New response evaluation criteria in solid tumours: revised RECIST guideline (version 1.1). Eur J Cancer 2009;45:228-47.

23. Cho H, Kim S, Jo K, Jeong YH, Kang WJ. Tumor Glucose Metabolism and Its Heterogeneity on F-18 FDG PET/CT Provide Better Prognostication in Nonmetastatic Human Papillomavirus-Related Oropharyngeal Squamous Cell Carcinoma. Cancers (Basel) 2021;13:5538.

24. Bray F, Ferlay J, Soerjomataram I, Siegel RL, Torre LA, Jemal A. Global cancer statistics 2018: GLOBOCAN estimates of incidence and mortality worldwide for 36 cancers in 185 countries. CA Cancer J Clin 2018;68:394-424.

25. Horgan AM, Amir E, Walter T, Knox JJ. Adjuvant therapy in the treatment of biliary tract cancer: a systematic review and meta-analysis. J Clin Oncol 2012;30:1934-40.

26. Maegawa FB, Hamdan M, Barrientes A, Philipovskiy A, Elhanafi S, Tyroch AH, Konstantinidis IT. Gallbladder Adenocarcinoma: the Impact of Tumor Location and Minimally Invasive Surgery on Survival. J Gastrointest Surg 2021;25:2104-6.

27. Han D, Yang J, Xu F, Huang Q, Bai L, Wei YL, Kaaya RE, Wang S, Lyu J. Prognostic factors in patients with gallbladder adenocarcinoma identified using competing-risks analysis: A study of cases in the SEER database. Medicine (Baltimore) 2020;99:e21322.

28. Yifan T, Zheyong L, Miaoqin C, Liang S, Xiujun C. A predictive model for survival of gallbladder adenocarcinoma. Surg Oncol 2018;27:365-72.

29. Yu T, Yu H, Cai X. Preoperative prediction of survival in resectable gallbladder cancer by a combined utilization of CA 19-9 and carcinoembryonic antigen. Chin Med J (Engl) 2014;127:2299-303.

30. Sachan A, Saluja SS, Nekarakanti PK, Nimisha, Mahajan B, Nag HH, Mishra PK. Raised CA19-9 and CEA have prognostic relevance in gallbladder carcinoma. BMC Cancer 2020;20:826.

31. Wen Z, Si A, Yang J, Yang P, Yang X, Liu H, Yan X, Li W, Zhang B. Elevation of CA19-9 and CEA is associated with a poor prognosis in patients with resectable gallbladder carcinoma. HPB (Oxford) 2017;19:951-6.

32. Kim HJ, Chang HS, Ryu YH. Prognostic Role of Pre-Treatment [18F]FDG PET/CT in Patients with Anaplastic Thyroid Cancer. Cancers (Basel) 2021;13:4228.

33. Weber WA, Schwaiger M, Avril N. Quantitative assessment of tumor metabolism using FDG-PET imaging. Nucl Med Biol 2000;27:683-7.

34. Geus-Oei LF, Oyen WJ. Predictive and prognostic value of FDG-PET. Cancer Imaging 2008;8:70-80.

35. Annunziata S, Pizzuto DA, Caldarella C, Galiandro F, Sadeghi R, Treglia G. Diagnostic accuracy of fluorine-18-fluorodeoxyglucose positron emission tomography in gallbladder cancer: A meta-analysis. World J Gastroenterol 2015;21:11481-8.

36. Furukawa H, Ikuma H, Asakura K, Uesaka K. Prognostic importance of standardized uptake value on F-18 fluorodeoxyglucose-positron emission tomography in biliary tract carcinoma. J Surg Oncol 2009;100:494-9.

37. Fendler WP, Philippe Tiega DB, Ilhan H, Paprottka PM, Heinemann V, Jakobs TF, Bartenstein P, Hacker M, Haug AR. Validation of several SUV-based parameters derived from 18F-FDG PET for prediction of survival after SIRT of hepatic metastases from colorectal cancer. J Nucl Med 2013;54:1202-8.

38. Cheng G, Huang H. Prognostic Value of (18) F-Fluorodeoxyglucose PET/Computed Tomography in Non-Small-Cell Lung Cancer. PET Clin 2018;13:59-72.

39. Yoo J, Choi JY, Lee KT, Heo JS, Park SB, Moon SH, Choe YS, Lee KH, Kim BT. Prognostic Significance of Volume-based Metabolic Parameters by (18)F-FDG PET/CT in Gallbladder Carcinoma. Nucl Med Mol Imaging 2012;46:201-6.

40. Lam R, Zakko A, Petrov JC, Kumar P, Duffy AJ, Muniraj T. Gallbladder Disorders: A Comprehensive Review. Dis

Mon 2021;67:101130.

41. Chun YJ, Jeung HC, Park HS, et al. Significance of Metabolic Tumor Volume and Total Lesion Glycolysis Measured Using ^{18}F-FDG PET/CT in Locally Advanced and Metastatic Gallbladder Carcinoma. Yonsei Med J 2019;60:604-10.